Available online on 15.04.2021 at http://jddtonline.info

Journal of Drug Delivery and Therapeutics

Open Access to Pharmaceutical and Medical Research

Open Access Full Text Article

Research Paper

Preparation, *In Vitro* characterization and stability studies of ropinirole lipid nanoparticles enriched hydrogel for treatment of neurodegeneration diseases

Kumara Swamy Samanthula, Ramesh Alli, Thirupathi Gorre*

Department of Pharmaceutics, Vaagdevi Pharmacy College, Bollikunta, Warangal, Telangana State, India

All authors contributed equal to this work

Article Info:

Article History:

Received 09 Feb 2021
Review Completed 23 March 2021
Accepted 30 March 2021
Available online 15 April 2021

Cite this article as:

Samanthula KS, Alli R, Gorre T, Preparation, *In Vitro* characterization and stability studies of ropinirole lipid nanoparticles enriched hydrogel for treatment of neurodegeneration diseases, Journal of Drug Delivery and Therapeutics. 2021; 11(2-s):66-75
DOI: http://dx.doi.org/10.22270/jddt.v11i2-s.4648

*Address for Correspondence:

Thirupathi Gorre, Department of Pharmaceutics, Vaagdevi Pharmacy College, Bollikunta, Warangal, Telangana State, India

Abstract

Ropinirole (RP), is a selective dopamine agonist that is used alone or with other medications to treat the symptoms of Parkinson's disease (PD). RP has low bioavailability of only about 50% due to the first-pass metabolism, and it requires frequent dosing during oral administration. The objective of the current research was to develop RP loaded solid lipid nanoparticles (RP-SLNs), nanostructured lipid carriers (RP-NLCs), and their corresponding hydrogels (RP-SLN-C and RP-NLC-C) that might improve efficacy in PD treatment. RP nanoparticles were prepared by homogenization aided probe sonication method and optimized based on particle size, polydispersity index (PDI), zeta potential (ZP), assay, entrapment efficiency, and i*n vitro* release studies. Optimized formulations were converted to hydrogel formulations using Carbopol 934 as a gelling polymer and optimized based on rheological and release characteristics. Optimized formulations were further evaluated using differential scanning calorimetry (DSC), powder X-ray diffractometry (PXRD), scanning electron microscopy (SEM), freeze-drying, and stability study at refrigerated and room temperatures. The optimized RP-SLN formulation showed particle size and entrapment efficiency of 213.5±3.8 nm and 77.9±3.1% compared to 190.6±3.7 nm and 85.7±1.7% for optimized RP-NLC formulation. PXRD supplemented and confirmed DSC results, RP was entrapped in a molecularly dispersed state inside the core of the lipid nanocarrier. Furthermore, RP loaded lipid nanocarriers revealed a spherical shape in SEM images. *In vitro* release studies demonstrated sustained release profiles for RP from SLNs, NLCs, and their hydrogels over 24 h and were stable over three months at 4ºC and 25ºC storage conditions.

Keywords: Parkinson's disease, Ropinirole, Solid lipid nanoparticles, Nanostructured lipid carriers, Hydrogel.

INTRODUCTION:

Parkinson's disease (PD) is the second most common age-related degenerative disease of the central nervous system and represents the most common movement disorder[1]. PD affects 1-2 per 1000 of the population at any time. PD prevalence is increasing with age and PD affects 1% of the population above 60 years[1]. PD is usually gradual, with symptoms becoming more severe over time[2]. About one million Americans are thought to have PD. This is more than those affected by multiple sclerosis (MS), muscular dystrophy (MD), and amyotrophic lateral sclerosis (ALS) combined. PD is characterized by tremor, rigidity, postural abnormalities, stooped posture, bradykinesia, akinesia, and festinating gait[3]. The significant pathological change in patients with PD is the loss of melanin-containing dopaminergic neurons in the zona compacta of the substantia nigra[4]. These pigmented neurons have been identified as nigrostriatal dopamine neurons; loss of these neurons results in a decrease of dopamine content in the striatum[5].

RP is a new non-ergoline D2/D3 dopamine receptor agonist, binds specifically to D2-receptors in striatum and substantia nigra, with selectivity similar to that of dopamine. It is supposed to induce its antiparkinsonian action via enhancing striatal neuronal dismissal rates through selective stimulation of D2-dopamine receptors. RP is also used for the treatment of restless leg syndrome. When taken as oral tablets, RP has poor oral bioavailability (~50%) due to extensive hepatic first-pass metabolism, with a plasma half-life of approximately 5.8 h and t_{max} which is less than one hour. Currently, RP conventional oral tablet dosage form with 3-9 mg tablet strength is available in the market, is showing low oral bioavailability. Intravenous administration is very irritating and is not recommended[6,7]. Therefore, alternative routes and drug delivery systems are required to improve its therapeutic outcomes. Further, RP can be administered as a monotherapy as well as combination therapy with levodopa because it can help in the reduction of the administered dose of levodopa. The continuous delivery of RP from the transdermal system may delay or prevent the onset of levodopa related motor complications due to continuous dopaminergic stimulation[8]. It could be anticipated that a once-daily regimen shall significantly increase patient compliance while at the same time reducing the burden of the caregiver[9]. Therefore, in the current

investigation transdermal route was selected as an alternative prime of the route of administration for RP.

A wide variety of transdermal drug delivery systems containing different drugs have been prepared, but their clinical application is limited by permeation barriers in the skin[10]. The primary drawback of the transdermal route is the highly unique organized anatomy of the skin. For many years, the main target was to exert a local effect on the skin[8, 9, 11]. Recently, drugs have been shown to achieve better therapeutic outcomes through the transdermal route than by oral administration. Diverse methodologies have been developed to facilitate the transdermal transport of therapeutic agents such as using penetration enhancers[12], iontophoresis[13], microneedles[14], and lipid vesicle carriers[15]. Moreover, many vesicular carrier systems including lipid nanoparticles such as SLNs NLCs[16, 17], Transfersomes[18], liposomes, niosomes and ethosomes[15, 19] has been investigated for topical application of different drugs.

SLNs and NLCs loaded hydrogels have been widely investigated for the enhanced skin penetration of drugs and to expand the range of molecules that can be used clinically in the dermatological formulation. SLNs are nano-sized colloidal carriers with 50-1000 nm size, composed of solid lipids with surfactants as stabilizing agents, and remain in the solid-state at room and body temperature[20, 21]. NLCs are the second generation of SLNs, in which a liquid lipid has been added to the solid lipid[22]. Both SLNs and NLCs can combine many advantages such as controlled release, large scale production, and toxicologically acceptable compared with other colloidal carrier systems[23, 24]. SLNs and NLCs applied for transdermal and dermatological applications due to their various desirable effects on the skin as well as their characteristics as colloidal carriers. They can be applied to damaged or inflamed skin because they are prepared with non-irritant and non-toxic lipids. Furthermore, these lipid nanoparticles showed occlusive properties as a result of film formation on the skin, which reduces transdermal water loss and also favored the drug penetration into the skin[23-2]. Moreover, SLN and NLC containing hydrogels have been reported for the enhanced skin penetration of various drugs such as triptolide, flurbiprofen, and RP[27-29].

The objective of the present study was to develop RP-SLN and RP-NLC formulations and their corresponding hydrogels (RP-SLN-C and RP-NLC-C) for enhanced therapeutic outcomes in the treatment of PD. Hence, RP-SLN and RP-NLC formulations were prepared by hot-melt emulsification coupled with probe sonication method and optimized based on physical characteristics, % assay, % entrapment efficiency, and in vitro release in comparison with RP hydrogel (RP-C) and RP suspension (RP-S) as control formulations. Optimized lipid nanoparticles were converted to hydrogels using Carbopol 934 as a gelling agent. Lipid nanoparticles and their hydrogel formulations were further evaluated for morphology, stability, and solid-state characterization.

MATERIALS AND METHODS

RP was a generous gift from Wockhardt Pharmaceuticals Pvt. Ltd., Aurangabad, India. Propylene glycol monocaprylate (Capryol® 90), tripalmitin (Dyanasn™ 114), Poloxamer 188, polyoxyethylene sorbitan monolaurate (Tween® 20), and Centrisart filters (10 kDa molecular weight) were purchased from Sigma Aldrich Chemicals Pvt Ltd., Bangalore, India. Carbopol® 934 was procured from Hi-Media, Mumbai, India. Other glassware and chemicals required for this project like High-Performance Liquid Chromatography (HPLC) grade solvents were obtained from Merck Hyderabad, India.

Quantification of RP by HPLC

RP was quantified based on an earlier published HPLC method with slight modification and subsequent validation[30]. The mobile phase consisted of a mixture of acetonitrile, phosphate buffer, and triethanolamine (58:42:0.3 %v/v) was adjusted at a pH of 6.0 with a flow rate of 1 ml/min. A C_{18} Phenomenex Luna® (250 mm x 4 mm, 5 µ) column was used for HPLC separation. The temperature for the analyses was 25°C, the injection volume was 20 µL, and the UV detection wavelength was set to 245 nm at Absorbance Units Full Scale (AUFS) 1.00. The modified method was linear over the concentration range of 2.5-50 µg/ml. The modified method was also found to be precise and accurate with a limit of detection (LOD) and limit of quantitation (LOQ) of 1.0 and 2.5 µg/mL, respectively.

Preparation of RP loaded lipid nanoparticles

RP-SLN and RP-NLC formulation was prepared by hot-melt emulsification coupled with probe sonication method[31, 32]. An aqueous phase was prepared using surfactants (Tween® 20 and Poloxamer 188) in bi-distilled Milli-Q water, and heated to 65±5°C. The oily phase consisted of RP (0.2 % w/v) dissolved in Dyanasn™ 114 and soylecithin mixture, heated at a temperature of 65±5°C during SLN preparation. For NLC preparation, the oily phase consisted of RP (0.2 % w/v) dissolved in Dyanasn™ 114, Capryol® 90, and soylecithin mixture. The hot aqueous phase was added to the molten oily phase drop by drop under constant magnetic stirring at 2000 rpm for 10 mins to form a homogeneous mixture. The formed emulsion was then further emulsified at 12,000 rpm for 10 mins using Diax 900 (Heidolph, Germany), to form a hot emulsion. The hot coarse emulsion was cooled to room temperature and subjected to probe sonication using12T probe sonicator (Vibracell, Sonics, CT, USA) for 15 min at 40% amplitude in an ice immersed beaker. Cooling this dispersion to room temperature led to the solidification of the solid lipid in both formulations and formation of the SLNs and NLCs.

Table 1: Composition of ropinirole loaded SLN, NLC, and control suspension formulations.

Ingredients (% w/v)	RP-SLN1	RP-SLN2	RP-SLN3	RP-SLN4	RP-NLC1	RP-NLC2	RP-NLC3	RP-NLC4	RP-S
RP	0.2	0.2	0.2	0.2	0.2	0.2	0.2	0.2	0.2
Dynasan® 114	1.0	1.5	2.0	3.0	2.0	1.5	1.25	1.5	-
Caproyl™ 90	-	-	-	-	0.75	0.5	0.75	0.75	-
Soylecithin	1.5	1.5	1.5	1.5	1.5	1.5	1.5	1.5	-
Poloxamer 188	1	1	1	1	1	1	1	1	-
Tween® 20	-	-	-	-	-	-	-	-	1
Water (mL)	10	10	10	10	10	10	10	10	10

RP suspension (RP-S)

RP suspension (RP-S) formulation was prepared by dissolving 20 mg of RP in 10 ml bi-distilled Milli-Q water containing Tween® 20 (1 % w/v) as a suspending agent under continuous magnetic stirring at 2000 rpm for 60 mins at room temperature. This preparation was used as a control for both RP-SLN and RP-NLC formulations.

Preparation of SLN and NLC enriched hydrogels

Gel formulations of RP-SLN and RP-NLC were prepared by using different concentrations of Carbopol 934 as a gelling agent. Initially, Carbopol was dispersed in double distilled water containing glycerol (10% w/v), after which this aqueous dispersion was soaked overnight for swelling. RP-SLN and RP-NLC formulations and the aqueous dispersion of the gelling agent were mixed in a high-speed stirrer (Remi, Mumbai, India), for 5 min at 100 rpm, to yield RP nanocarrier loaded hydrogels. Triethanolamine (0.3% w/v) was added to neutralize the pH of the hydrogel formulations for topical application range. The prepared hydrogels were left overnight to remove any entrapped air.

Table 2: Composition of ropinirole lipid nanoparticles enriched hydrogels

Ingredients (% w/v)	RP-SLN-C1	RP-SLN-C2	RP-SLN-C3	RP-SLN-C4	RP-NLC-C1	RP-NLC-C2	RP-NLC-C3	RP-NLC-C4	RP-CS
RP	0.2	0.2	0.2	0.2	0.2	0.2	0.2	0.2	0.2
Dynasan® 114	2.0	2.0	2.0	2.0	1.25	1.25	1.25	1.25	-
Caproyl™ 90	-	-	-	-	0.75	0.75	0.75	0.75	-
Soylecithin	1.5	1.5	1.5	1.5	1.5	1.5	1.5	1.5	-
Poloxamer 188	1	1	1	1	1	1	1	1	-
Carbopol 934	0.5	0.75	1.0	1.25	0.5	0.75	1.0	1.25	1
Tween® 20	-	-	-	-	-	-	-	-	1
Water (mL)	10	10	10	10	10	10	10	10	10

RP hydrogel (RP-C)

The conventional RP-C formulation was prepared similarly like SLN and NLC containing hydrogels with the same RP concertation.

Characterization of RP-SLN and RP-NLC

Particle Size (PS), Polydispersity index (PDI), and Zeta potential (ZP)

PS, PDI, and ZP of the prepared nanoparticles were analyzed, using a photon correlation spectroscopy with Malvern Zetasizer (Nano ZS90, UK). For the measurement of PS and PDI, the prepared lipid nanoparticles were diluted 50 times with double distilled water to get optimum Kilo Counts per Second for measurements. ZP of the formulations was measured with the same diluted sample, using an electrode cell based on the Smoluchowski equation. All measurements were carried out at 25ºC in triplicate[33].

Total RP content

An accurately measured volume of RP-SLN and RP-NLC (100 µL) was extracted in ethanol (990 µL) because RP is soluble in ethanol. The ethanol-formulation mixture was then vortexed for 5 mins at 5000 rpm. Mixtures were further diluted with the mobile phase[34]. The diluted samples were analyzed for RP content with HPLC. The RP drug content was used in the determination of the percentage of RP entrapped in the nanoparticles.

RP Entrapment efficiency (EE)

EE was determined by measuring the concentration of the unentrapped (free drug) in the aqueous medium based on an earlier reported experiment[35]. The aqueous medium was separated by ultra-filtration using centrisart tubes (Sartorius, Goettingen, Germany), which consisted of a filter membrane (MWt. cut off 20 kDa) at the base of the sample recovery chamber. A measured volume of the formulations (2.5 mL) was taken and placed in the outer chamber, and the sample recovery chamber was placed on top of the sample and centrifuged (Remi, India) for 15 mins at 15000 rpm. The filtrate was collected and analyzed for free RP by HPLC after proper dilution with ethanol. The EE of RP in nanoparticles was calculated based on the following formula:

$$\% \text{ EE} = \left[\frac{\text{Amount of RP determined in drug content experiment} - \text{amount of unentrapped RP}}{\text{Amount of RP weighed}}\right] \text{X100} \quad (1)$$

In vitro release studies

In vitro release of RP from the respective formulations such as with RP-S, RP-SLN, and RP-NLC formulations were evaluated using Franz diffusion cells. Dialysis membrane (pore size of 2.4 nm, a diameter of 72 dm, 12,000 -14,000 K MWCO, Hi-Media, Mumbai, India) was soaked overnight in double distilled water before the *in vitro* release studies[10]. The dialysis membrane was mounted on diffusion cells between donor and receptor chambers and fastened with clamps. The temperature of the cells was maintained at 37±0.5°C. Twelve milliliters of Phosphate buffer (PB - pH 6.8) was used as the receptor media during the course of the experiment[37]. 0.5 mL of each formulation was added into the donor chamber. At predetermined time points, aliquots (1 mL) were withdrawn from the receiver chamber and replaced with an equal volume of the Phosphate buffer (PB - pH 6.8) solution. The collected samples were analyzed for RP content using HPLC. RP release data were kinetically analyzed to study the possible mechanisms of drug release using Kinet DS3 software. Linear regression equations were used, and the coefficient of determination (R^2) was calculated[38, 39] (Ref 38, 39).

Evaluation of RP-SLN-C and RP-NLC-C

A. Homogeneity:

All developed hydrogels were tested by visual inspection after the gels have been set in the container. They were tested for their homogeneity, consistency, and presence of lumps.

B. pH:

The pH of the prepared hydrogel formulation was determined using a digital pH meter (PH540GLP, WTW, Germany) in triplicate at 25ºC. One gram of the hydrogel was dispersed in 10 mL of distilled water before measurement.

C. Viscosity:

The viscosity of hydrogels was measured at 25ºC, using a Brooke field viscometer DV-II model with a T-Bar spindle of T-64 in combination with a helipath stand. One gram of the hydrogel was dispersed in 10 mL of distilled water in a glass beaker. The helipath T-bar spindle was moved up and down, giving viscosities at the number of points along the path[40].

D. Spreadability:

Generally, time in seconds taken by both glass slides to slip-up off from hydrogel formulation placed in between the slides under the direction of a certain load is considered as spreadability of the formulation. An accurately weighed amount of prepared hydrogel formulation (1 g) was placed between two glass slides and known weight placed over an upper glass slide and left for about 5 min[41]. The time required by the upper slide to move on the application of weight to it through the pulley was noted, and spreadability was calculated by using the following formula (3), in triplicate:

$$S = W \times L/T \qquad (2)$$

Where S - Spreadability; W - Weight applied above upper slide; L - Length of the glass slide and T - Time is taken to separate the slides from each other.

E. Extrudability:

The extrudability test is used to determine the force essential to extrude the gel from the packed tube container. For this purpose, a known amount of gel formulation was filled in a standard capped collapsible aluminum tube and sealed by crimping both ends. The weight of the tube was recorded. Then the tubes were placed between the two glass slides were clamped. A 500 g of weight was placed over the glass slides, and the cap was removed. The amount of gel extruded was collected and weighed[42]. The extrudability of each formulation was measured, in triplicate, and calculated by using the formula (4):

$$E = W/A \qquad (3)$$

Where, E - Extrudability, W - Applied weight to extrude gel from the tube, and A - Area

F. Drug content:

An accurately weighed amount of RP-SLN-C and RP-NLC-C (0.5 g) was dissolved in ethanol (15 ml). The ethanol-formulation mixture was then vortexed for 5 mins at 5000 rpm, sonicated in a bath sonicator (Sonica, 3200MH, Germany) for 15 min to get complete solubility of the drug. The analyte was prepared and estimated for drug content as per the drug content procedure of lipid nanoparticles.

G. *In vitro* release:

A similar release study was performed as per the lipid nanoparticles release study: however, 0.5 g hydrogel was added to the donor chamber.

Lyophilization of RP-SLN and RP-NLC formulations

Optimized RP-SLN and RP-NLC formulations were subjected to a freeze-drying process. Trehalose dihydrate was used as a cryoprotectant (10% w/w) and added to the aqueous phase during the preparation of nanoparticles. Prepared formulations were kept overnight in an ultra-freezer at -80ºC (Sanyo, Japan). The frozen samples were then transferred into a freeze-dryer (Lyodel, Delvac Pumps Pvt. Ltd, India). A vacuum was applied, after which the sample was subjected to various drying phases for about 36 h to get powdered RP-SLN and RP-NLC[36, 43]. Freeze-dried formulations were reconstituted with water and used for further experimental studies.

Solid-state characterization

A. Differential scanning calorimetry (DSC):

A differential scanning calorimeter (DSC 822 e/200, Mettler, Switzerland) was employed to observe both the melting and recrystallization behavior of RP in the absence and presence of other excipients within different formulation (pure RP, pure solid lipid, physical mixture of drug and Dynasan®114 (1:1) and lyophilized RP-SLN3 and RP-NLC3 formulations). Initially, the instrument was calibrated with indium (calibration standard, purity > 99.99%). Eight to ten milligrams of the sample, individually sealed in the standard aluminum pans, was placed over the sample platform. A reference pan (empty sealed aluminum pan) was placed simultaneously on the reference platform. The two pans were heated from 30 to 300ºC at a rate of 10ºC/min under a nitrogen purge[44].

Powder X-Ray Diffraction Analysis (PXRD):

A qualitative PXRD analysis was performed to examine the physical state of RP in pure RP powder, pure solid lipid, physical mixture of Dynasan®114 lipid and RP, and freeze-dried formulated RP-SLN and RP-NLC using a powder X-ray diffractometer (PXRD 6000, Shimadzu, Japan). In this technique, the samples were exposed to nickel filtered CuKα radiation (40 kV, 30 mA) and scanned from 2° to 50°, 2θ at a step size of 0.045° and step time of 0. 5 s.

B. Scanning electron microscopy (SEM) for lipid nanoparticles and their hydrogels:

Lipid nanoparticulate formulations and their corresponding hydrogels were characterized by scanning electron microscope (S4800, Hitachi, Japan; SEI, Hitachi, Japan). Briefly, the formulation was mounted on a carbon-coated brass stub. This was sputter-coated with a Platinum coating machine (JEOL, JFC-1600 Auto fine coater) and mounted in SEM for surface analysis by applying different voltage[45].

Stability studies

Physico-chemical stability of the optimized RP-SLN, RP-NLC formulations, and their corresponding optimized hydrogels was evaluated during the storage of formulations at refrigerated (4±2ºC) and room temperature (25±2ºC) for three months. RP-SLN and RP-NLC formulations were stored in 20 ml scintillation glass vails while RP-SLN-C and RP-NLC-C hydrogels were filled in aluminum collapsible tubes. Samples were withdrawn from RP-SLN and RP-NLC formulations at predetermined time intervals and analyzed for physical parameters such as PS, PDI, ZP, % EE, and assay while RP-SLN-C and RP-NLC-C formulations were observed for the change in pH, viscosity, spreadability, extrudability, and % drug content[28, 46].

Statistical analysis

Unpaired student t-test using Graph pad prism software (version 5. 02.2013, USA) was employed to analyze the differences between groups. Data obtained was considered to be statistically significant at the level of ($p<0.05$).

RESULTS AND DISCUSSION

Dynasan® 114, Caproyl™ 90, soylecithin, and Poloxamer 188 were selected as solid lipid, liquid lipid, primary and secondary surfactant, respectively for the preparation of RP-SLN and RP-NLC formulation, based on earlier reported solubility studies as well as screening studies. Process parameters such as homogenization time and speed, probe sonication time, and amplitude were optimized based on physical characteristics and stability criteria. Homogenization alone does not reduce the PS for the ideal transdermal application. Homogenization coupled with probe sonication yielded the nanoparticles with the desired transdermal application range (data not shown). Homogenization time and speed at 12000 rpm for 10 mins, probe sonication for 15 mins at 40% amplitude were selected as the optimized process parameters for the preparation of both RP-SLN and RP-NLC formulations and their corresponding hydrogels. RP-SLN is composed of Dynasan® 114 as the solid lipid and RP-NLC is composed of Dynasan® 114 and Caproyl™ 90 as the solid and liquid lipid, respectively. Solid to liquid lipid ratio 3:1 has been reported as a general ideal ratio for the preparation of NLCs[31].

Characterization of RP-SLN and RP-NLC formulations

PS, PDI, and ZP

The composition of all prepared SLN and NLC formulations is shown in Table 1. Both types of formulation were prepared and evaluated for Physico-chemical characteristics (PS, PDI, ZP, % assay, and % EE) as shown in Table 3. PS significantly increased with increasing solid lipid concentration. A huge increase in PS was observed at 3% solid lipid concentration that may be due to the sonication energy is more efficient in dilute dispersion (RP-SLN1) than the concentrated dispersion (i.e., higher lipid concentration, RP-SLN4). In the case of NLCs, PS decreased with decreasing the ratio between solid and liquid lipids in the formulation. RPNLC3 prepared at 1.7:1 solid to liquid lipid ratio showed significantly lower PS than other combinations, even lower than RP-SLN3, containing one solid lipid at the same lipid percentage (2% w/v). Similar results were reported by Puglia, *et al*. and Corinne eta l. reported that the addition of liquid lipid to solid lipid tends to decrease PS, which could be due to increasing in molecular mobility of the matrix after liquid oil addition[47, 48] . However, different results were reported by Soleimanian *et al.* who suggested that PS increase by increasing the liquid lipid concentrations could be due to the more disordered crystalline structure inside the nanoparticles[49]. PDI of both formulations was below 0.5 which confirms the homogeneous distribution of the formulations[50]. In the case of SLNs, higher PDI at lower lipid concentration could be due to higher drug to lipid ratio as drug concentration remained the same. ZP is a good indicator to predict the physical stability of the SLN and NLC dispersions[51]. Nano-dispersions have ZP values less than -20 mV, predicts good physical stability of nanoparticle dispersion. Therefore, all of the nanocarrier dispersions prepared are expected to be stable[52]. The presence of Poloxamer 188, a non-ionic surfactant, which promotes the steric stabilization because it can reduce the electrostatic repulsion between the particles by establishing a coat around the surface for keeping the stability of lipid nanoparticles[20]. RP-SLN3 and RP-NLC3 showed PS, PDI, ZP of 213.5±3.8 nm, 0.22±0.07, -29.3±2.0 mV and 190.6±2.1 nm, 0.19±0.06 and -29.8±1.6 mV, respectively. All nanocarrier formulations showed PS below 250 nm which is ideal for the application of topical route[53].

Table 3: Particle size, Polydispersity index, Zeta potential, % assay and % entrapment efficiency ropinirole loaded SLN and NLC formulations (mean ± SD, n=3).

Formulation	PS	PDI	ZP (mV)	Assay (%)	EE (%)
RL-SLN1	174.3±4.5	0.35±0.08	-26.3±1.1	92.8±2.0	70.2±1.5
RP-SLN2	189.6±2.9	0.28±0.05	-27.9±1.5	97.3±205	72.3±2.4
RP-SLN3	213.5±3.8	0.22±0.07	-29.3±2.0	98.6±1.8	77.9±3.1
RP-SLN4	247.9±5.7	0.28±0.04	-27.4±1.3	96.3±3.2	74.3±1.2
RP-NLC1	220.4±4.4	0.20±0.04	-26.8±2.1	94.3±2.8	79.4±1.5
RP-NLC2	205.9±2.5	0.24±0.07	-24.9±3.0	96.7±1.6	81.0±1.5
RP-NLC3	190.6±3.7	0.19±0.06	-29.8±1.6	99.1±3.1	85.7±1.7
RP-NLC4	214.7±3.3	0.22±0.05	-27.5±2.5	96.9±1.9	82.6±3.6

Drug content and EE

Drug content and EE of the RP-SLN and RP-NLC formulations are shown in Table 3. In the case of SLNs, EE increased with increasing lipid concentration which could be due to a higher amount of lipid was existing to encapsulate more drug molecules at higher lipid concentration. EE of the RP-SLN3 was found to be 77.9± 3.1% which is less than RP-NLC3 (85.7±1.7%). In general, drugs are more soluble in liquid lipids than solid lipids which help in increasing EE. The addition of liquid lipids to solid lipids reduces the crystallinity and increases imperfections in the crystal lattice which leaves enough space to accommodate more drug molecules, thus, results in enhanced loading capacity and drug EE[54].

In vitro release

The *in vitro* drug release profiles of RP-loaded SLNs and NLCs are shown in Figure 1A. To evaluate the controlled release potential of all prepared formulations, the release of RP from the lipid nanoparticles was investigated for 24 h. In the case of SLNs, the maximum amount of RP release was from RP-SLN1 formulation compared to other SLN formulations; which could be due to low solid lipid concentration in the formulation. RP-SLN1 formulation (94.0%) and RP-SLN2 formulation (93.4%) showed maximum RP release in 18 h, whereas for RP-SLN3 formulation (84.3%) and RP-SLN4 formulation (60%) showed maximum RP release in 24 h. In the initial 2 h, the RP release was less than 20% from all formulations and increased with time. This could be due to the slow diffusion

of RP from the lipid matrix. This liquid lipid-enriched shell possessed soft character and considerable high solubility for lipophilic drugs[23, 24, 55], in which RP was easily loaded to higher amounts. In the case of NLCs, RP-NLC1 formulation (93.0%) and RP-NLC2 formulation (92.8%) showed maximum RP release in 18 h, whereas for RP-NLC3 formulation (92.3%) and RP-NLC4 formulation (68%) showed maximum RP release in 24 h. The incorporation of liquid lipids into the crystalline matrix made NLC imperfect and allowed loaded RP to be released easily, thus increasing % RP release when liquid lipid was included in the NLC matrix. RP-S formulation showed 96.7 ± 2.8 % RP release over 12 h. This suggested a sustained release profile RP from the lipid nanocarriers[56].

The *in vitro* drug release profiles of RP nanocarrier-loaded hydrogels are shown in Figure 1B. RP-C formulation showed maximum RP release (99.1 ± 2.3%) in 18 h and demonstrated a significant different RP release profile than other eight hydrogel formulations. Furthermore, the presence of the surrounding Carbopol 934 hydrogel did not have a profound effect on the release profiles of SLN and NLC nanocarriers as shown in Figure 1B. These sustained release profiles cannot be attributed to drug diffusion through the Carbopol 934 hydrogel matrix, because the release of RP alone (no nanocarriers) from Carbopol 934 was complete in 18 h. The RP release from the hydrogel formulations was relatively slow compared with SLN and NLC nanocarriers. This could be due to the fact that RP was entrapped in the crystalline lipid matrix which was in turn dispersed into the hydrogel matrix.

The mathematical model showed the highest R^2 value was considered the best model to describe release kinetics. The data were fitted into Zero-order, First-order, Higuchi, and Korsmeyer-Peppas models. The high R^2 values were observed with Korsmeyer-Peppas 0.98, with n (slope) values above 0.5 for RP-SLN-C3 and RP-NLC-C3 formulations. This suggested that the release of drug from lipid nanocarriers as well as nanocarrier containing hydrogel formulations followed a non-Fickian with anomalous diffusion mechanism (diffusion and erosion)[57-62]. Based on physico-chemical characterization and *in vitro* release studies, RP-SLN3 and RP-NLC3 formulations were selected as the optimized formulations for further evaluation.

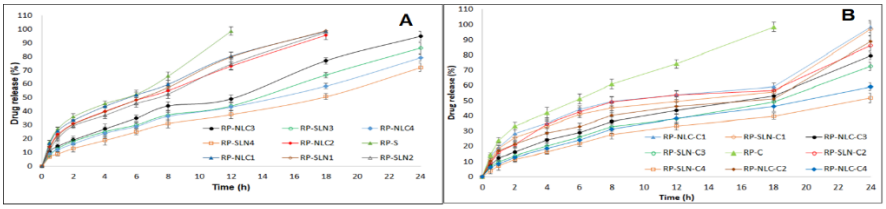

Figure 1: Release profiles of ropinirole from drug-loaded lipid nanocarriers (A) and hydrogels (B) formulations through the dialysis membrane (mean ± SD, n=3).

Characterization of SLN- and NLC-containing hydrogels

RP was maintained at 0.2% w/v concentration in all hydrogel formulations as shown in Table 2. Moreover, all prepared gel formulations were neutralized by triethanolamine (0.3% w/v). Triethanolamine is a non-ionic neutralizer that did not disrupt the ionic balance, thus, there was no aggregation observed for the prepared nanocarrier loaded hydrogels. Therefore, ionic neutralizers were not used in the present study[47].

A. Homogeneity:

RP-SLN3 and RP-NLC3 containing hydrogel formulations were kept aside for 24 h and observed for color, odor, and consistency. All developed gels were homogenous with the absence of lumps as presented in Table 4. They did not also show any signs of sedimentation after centrifugation.

B. pH:

The pH of all hydrogels was measured by a digital pH meter as presented in Table 4. The pH of all developed hydrogel formulations was neutralized by the addition of triethanolamine and ranged from 6.1 to 6.5 which is ideal pH for dermal applications[48, 63].

C. Viscosity:

Rheological characteristics are crucial physical parameters in the preparation of a potential drug delivery vehicle for topical application. The viscosity of the hydrogels is an essential parameter for dermal and topical hydrogels. Developed hydrogels are required to exhibit appropriate viscosities to circumvent delayed drug release with high viscosity preparations or difficulties in keeping the contact between the skin and hydrogels with low viscosity preparations. Table 4 provides information about the viscosity of all developed hydrogels. Increasing Carbopol 934 concentration resulted in a simultaneous increase in viscosity of the formulation.

D. Spreadability:

The spreadability of the drug delivery system permits easier application and provides more surface area available for drug penetration. The spreadability of RP-SLN-C3 and RP-NLC-C3 formulations was 6.7±0.4 g.cm/sec and 6.0±0.3 g.cm/sec, respectively. This suggests the simple application of the formulation of a hydrogel, with the use of slight shear on the surface of the skin. Increasing hydrogel viscosity had a negative effect on spreadability as shown in Table 4.

E. Extrudability:

The work required for extruding the preparation from the tube is known as extrudability. Spreadability and extrudability are the essential texture parameters, influencing patient compliance. The extrudability of hydrogel formulations was found to increase with increasing Carbopol concentration as shown in Table 4. Extrudability was found to be 1.5±0.2 and 1.4±0.3 g/cm^2 RP-SLN-C3 and RP-NLC-C3 formulations, respectively, in 10 s on applying a weight of 500 g. The results were consistent with earlier reported studies[38]. In general, the more the gel is extruded, the better was the extrudability; hereafter, less energy was needed to extrude the gel from the filled container.

Table 4: pH, viscosity, % drug content, spreadability and extrudability of RP-SLN-C and RP-NLC-C hydrogel formulations (mean ± SD, n=3).

Parameter	Formulation							
	RP-SLN-C1	RP-SLN-C2	RP-SLN-C3	RP-SLN-C4	RP-NLC-C1	RP-NLC-C2	RP-NLC-C3	RP-NLC-C4
pH	6.1 ± 0.2	6.3 ± 0.4	6.5 ± 0.3	6.2 ± 0.5	6.2 ± 0.3	6.4 ± 0.2	6.5 ± 0.3	6.1 ± 0.2
Viscosity (cP)	835.6 ± 76.0	1858.6 ± 88.9	2537.8 ± 104.7	3647.6 ± 153.4	756.7 ± 40.5	1546.7 ± 74.7	2274.6 ± 99.3	3075.7 ± 101.4
Drug content	97.1 ± 3.2	97.0 ± 2.5	98.6 ± 1.7	95.8 ± 2.6	98.3 ± 1.5	99.1 ± 2.2	99.4 ± 1.7	96.9 ± 3.5
Spreadability (g cm/sec)	2.1 ± 0.09	4.2 ± 0.6	6.7 ± 0.4	7.3 ± 0.5	1.7 ± 0.3	3.9 ± 0.3	6.0 ± 0.3	6.9 ± 0.4
Extrudability (g/cm^2)	-	1.8 ± 0.3	1.5 ± 0.2	2.6 ± 0.5	-	1.5 ± 0.3	1.4 ± 0.3	3.1 ± 0.2

F. Drug content:

RP content was 98.6±1.7 and 99.4±1.7% in RP-SLN-C3 and RP-NLC-C3 formulations, respectively as presented in Table 4. Based on characterization studies of all developed nanocarrier-containing hydrogels and *in vitro* release studies, RP-SLN-C3 and RP-NLC-C3 formulations were selected as the optimized formulations for further evaluation.

Stability studies

Stability of RP loaded lipid nanocarriers and their corresponding hydrogel formulations were established by the storage of the optimized formulations at refrigerated and room temperature for three months. The effect of storage conditions on PS, PDI, ZP, % assay, and % entrapment efficiency of optimized formulations at refrigerated and room temperature not showed no significant changes in the physico-chemical parameters over three months. An insignificant difference (2-3%) was noticed at room temperature compared with the refrigerated temperature.

Lyophilization of RP containing SLN and NLC formulations

Lyophilization is a promising technique to increase the stability of lipid nanoparticles for an extended period of time. Moreover, transformation into powder form offers possibilities of incorporating lipid nanoparticles into pellets, tablets, and capsules and is used for the solid-state characterization and morphology studies[64]. The diluted lipid nanoparticle dispersions have a specific surface area and higher sublimation velocities. In this regard, a cryoprotectant such as Trehalose dihydrate was necessary to warrant redispersion without any aggregation. Cryoprotectants can interact with the polar head of the surface-active agents and assist as a kind of 'pseudo hydration shell[65]. RP-SLN3 and RP-NLC3 formulation formed a clear floppy cake without any sticking or moisture content. The lyophilized powder was reconstituted with the same concentration of RP in lipid nanoparticle dispersion and analyzed for Physico-chemical characteristics. PS and PDI of the reconstituted powders were increased by 2-fold compared with the values of the original formulation as shown in Table 5. However, no significant changes were observed in ZP, % drug content, and % EE of the lyophilized formulations. The changes in PS and PDI could be due to the aggregation of the particles by the process of lyophilization. These results came in accordance with earlier reported studies[51, 52].

Table 5: Effect of lyophilization on particle size, polydispersity index, Zeta potential, % assay, and % entrapment efficiency of optimized RP-SLN and RP-NLC formulations (mean ± SD, n=3)

Parameter	RP-SLN3		RP-NLC3	
	Pre-lyophilization	Post-lyophilization	Pre-lyophilization	Post-lyophilization
Size (nm)	218.9±5.1	398.6±10.3	198.6±4.2	402.9±2.3
PDI	0.21±0.08	0.36±0.04	0.20±0.08	0.35±0.08
ZP (mV)	-28.9±0.8	-29.0±3.1	-30.5±1.8	-28.6±1.1
Assay (%)	98.9±1.2	97.3±1.7	99.0±2.1	96.9±1.7
EE (%)	78.1±1.8	76.7±2.0	84.3±1.9	82.9±2.1

Solid-state characterization

A. DSC

DSC has been performed and thermograms of pure RP, pure solid lipid (Dynasan® 114), physical mixture, and optimized RP-SLN and RP-NLC powders were depicted in **Figure 2A**. DSC technique was used to determine the crystallinity and compatibility of RP with other formulation ingredients. RP showed a single prominent sharp endothermic peak at about 244.6ºC which indicates the crystalline nature of pure RP (243 – 255ºC)[66]. Similarly, the endothermic peak of the physical mixture showed RP melting peak at 243.5ºC. The absence of the sharp endothermic peak within the melting range of RP in SLN and NLC powder confirms the conversion of the crystalline state of the RP to an amorphous state. However, Dynasan® 114 showed a single sharp endothermic peak at 58.6 ºC in pure lipid, physical mixture, RP-SLN3, and RP-NLC3 powder thermograms.

B. PXRD

PXRD patterns of pure RP, pure lipid (Dynasan® 114), physical mixture of drug and the solid lipid, and lyophilized RP-SLN3 and RP-NLC3 formulations are shown in Figure 2B. PXRD spectrum of pure RP demonstrated numerous characteristic intense peaks at 2Θ values of 7.41, 11.56, 22.49, 23.73, 24.85, and 26.88 that indicates the crystalline nature of RP[29]. Although the unique peaks of RP were absent in the lyophilized sample, they were present with less intensity in the physical mixture. In this regard, RP was not in the crystalline state after the freeze-drying of lipid nanoparticles. The diffraction patterns of SLN and NLC formulations were comparable to the solid lipid, Dynasan® 114. However, the intensity of pure Dynasan® 114 peaks was reduced in the lyophilized powders[67]. This reduced intensity suggests the decreased crystallinity of lipids. The change in the crystallinity of lipid and drug could affect the release of RP from nanoparticles. This reduction came in correlation with the DSC data.

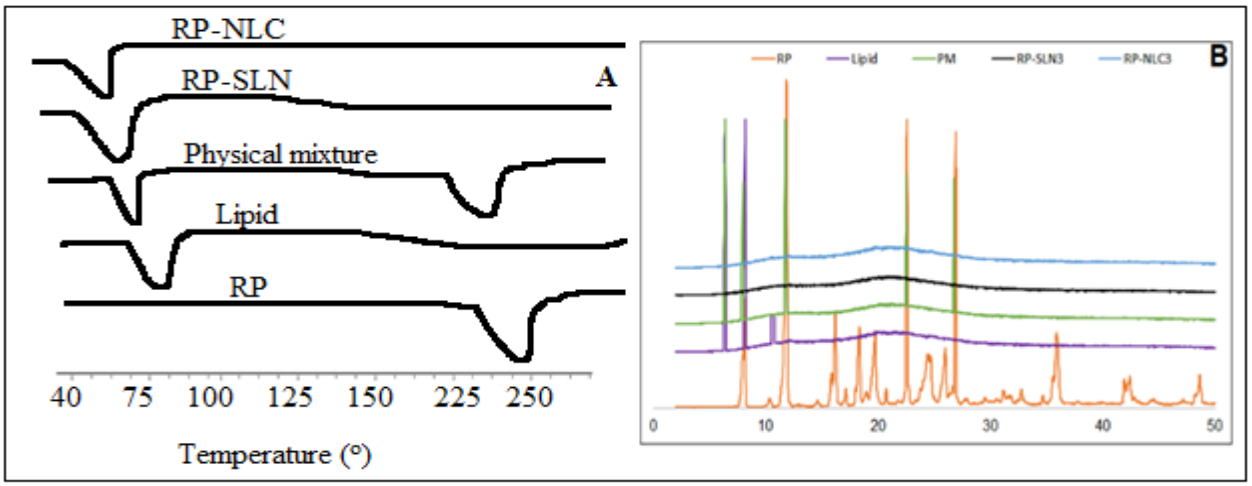

Figure 2. DSC thermograms (A) and Powder X-ray diffraction (B) of pure ropinirole, pure Dynasan® 114, physical mixture, lyophilized RP-SLN3, and RP-NLC3 formulations.

C. SEM

Figure 3A&3B represents the SEM micrographs of RP-SLN3 and RP-NLC3 powders that demonstrated a virtually sphere-shaped surface with aggregates along the particle surface. This particle aggregation could be due to the sticky nature of the lipid. The surface morphology of both RP-SLN3 and RP-NLC3 powders was smooth and there was no visible difference between them. However, hydrogel SEM micrographs demonstrated an uneven surface with higher scuffle boundaries as shown in Figure 3C&3D. The SEM images reveal that RP loaded nanoparticles were entrapped in the Carbopol hydrogel matrices, which is correlated with the sustained release profiles of the hydrogels[68,69,70].

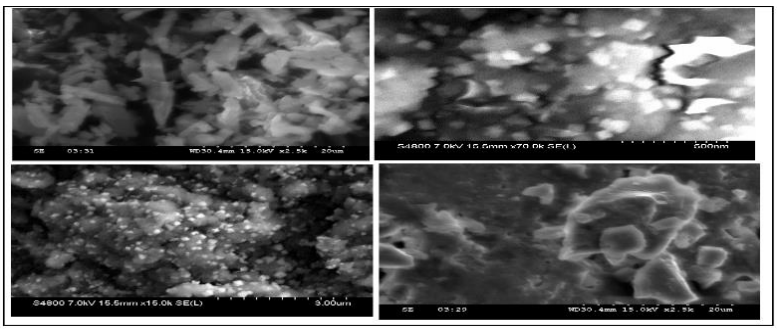

Figure 3: SEM micrographs of (A) RP-SLN3 powder, (B) RP-NLC3 powder, (C) RP-SLN-C3 hydrogel, and (D) RP-NLC-C3 hydrogel.

CONCLUSION

RP loaded SLN, NLC, and their corresponding hydrogel formulations were successfully developed and optimized. RP-SLN, RP-NLC, and their corresponding hydrogel formulations were stable over three months at refrigerated and room temperatures. *In vitro* release studies showed sustained release profiles of RP from all developed formulations. Therefore, the results demonstrated that SLN, NLC, SLN-, and NLC-enriched hydrogel formulations could serve as topical platforms for the transdermal delivery of RP for the effective management of Parkinsonism.

REFERENCES

1. De Lau LM, Breteler MM. Epidemiology of Parkinson's disease. The Lancet Neurology. 2006 Jun 1; 5(6):525-35.
2. McGregor MM, Nelson AB. Circuit mechanisms of Parkinson's disease. Neuron. 2019 Mar 20; 101(6):1042-56.
3. Tysnes OB, Storstein A. Epidemiology of Parkinson's disease. J Neural Transm. 2017; 124:901–905, doi:10.1007/s00702-017-1686-y.
4. Baul HS, Rajiniraja M. Favorable binding of quercetin to α-synuclein as potential target in Parkinson disease: an insilico approach. Research Journal of Pharmacy and Technology. 2018 Jan 31; 11(1):203.
5. Prasad J, Netam AK, Singh R, Sahu M, Satapathy T, Rao SP, Baghel P, Sahu MK. Therapeutic Approaches for the Management of Parkinson's Disease. Research Journal of Pharmacology and Pharmacodynamics. 2019 Feb 27; 11(1):46-52.
6. Pahwa R, Lyons KE, Hauser RA. Ropinirole therapy for Parkinson's disease. Expert review of neurotherapeutics. 2004 Jul 1; 4(4):581-8.
7. Shill HA, Stacy M. Update on ropinirole in the treatment of Parkinson's disease. Neuropsychiatric disease and treatment. 2009; 5:33.
8. Matheson AJ, Spencer CM. Ropinirole. Drugs. 2000 Jul 1; 60(1):115-37.
9. Raghubabu K, Jagannadharao V, Ramu BK. Assay of ropinirole hydrochloride in pharmaceutical preparations by visible Spectrophotometry. Asian Journal of Pharmaceutical Analysis. 2012 Jun 28; 2(2):41-5.
10. Prausnitz MR, Mitragotri S, Langer R. Current status and future potential of transdermal drug delivery. Nature reviews Drug discovery. 2004 Feb; 3(2):115-24.
11. Ulbrich K, Hekmatara T, Herbert E, Kreuter J. Transferrin-and transferrin-receptor-antibody-modified nanoparticles enable drug delivery across the blood–brain barrier (BBB). European Journal of Pharmaceutics and Biopharmaceutics. 2009 Feb 1; 71(2):251-6.
12. Heather AE. Benson, 2005. Transdermal Drug Delivery: Penetration Enhancement Techniques. Current Drug Deli.; 2:23-33.
13. Fatima T, Ajjarapu S, Shankar VK, Rangappa S, Shivakumar HN, Biswas SK, Hoque M, Murthy SN. Topical pilocarpine formulation for diagnosis of cystic fibrosis. Journal of pharmaceutical sciences. 2020 May 1; 109(5):1747-51.
14. Hussain MT, Forbes N, Perrie Y, Malik KP, Duru C, Matejtschuk P. Freeze-drying cycle optimization for the rapid preservation of protein-loaded liposomal formulations. International journal of pharmaceutics. 2020 Jan 5; 573:118722.
15. Dudhipala N, Phasha Mohammed R, Adel Ali Youssef A, Banala N. Effect of lipid and edge activator concentration on development of aceclofenac-loaded transfersomes gel for transdermal application: in vitro and ex vivo skin permeation. Drug development and industrial pharmacy. 2020 Aug 2; 46(8):1334-44.
16. Tatke A, Dudhipala N, Janga KY, Balguri SP, Avula B, Jablonski MM, Majumdar S. In situ gel of triamcinolone acetonide-loaded solid lipid nanoparticles for improved topical ocular delivery: Tear kinetics and ocular disposition studies. Nanomaterials. 2019 Jan; 9(1):33.
17. Dudhipala N, Youssef AA, Banala N. Colloidal lipid nanodispersion enriched hydrogel of antifungal agent for management of fungal infections: Comparative in-vitro, ex-vivo and in-vivo evaluation for oral and topical application. Chemistry and Physics of Lipids. 2020 Nov 1; 233:104981.
18. Janga KY, Tatke A, Dudhipala N, Balguri SP, Ibrahim MM, Maria DN, Jablonski MM, Majumdar S. Gellan gum based sol-to-gel transforming system of natamycin transfersomes improves topical ocular delivery. Journal of Pharmacology and Experimental Therapeutics. 2019 Sep 1; 370(3):814-22.
19. Kishan V, Shruthi K, Narendar D, Arjun N. Development and antimicrobial evaluation of binary ethosomal topical gel of terbinafine hydrochloride for the treatment of onychomycosis. International Journal of Pharmaceutical Sciences and Nanotechnology. 2018 Jan 31; 11(1):3998-4006.
20. Müller RH, Mäder K, Gohla S. Solid lipid nanoparticles (SLN) for controlled drug delivery–a review of the state of the art. European journal of pharmaceutics and biopharmaceutics. 2000 Jul 3; 50(1):161-77.
21. Dudhipala N. A comprehensive review on solid lipid nanoparticles as delivery vehicle for enhanced pharmacokinetic and pharmacodynamic activity of poorly soluble drugs. International Journal of Pharmaceutical Sciences and Nanotechnology. 2019 Mar 31; 12(2):4421-40.
22. Dudhipala N, Ay AA. Amelioration of ketoconazole in lipid nanoparticles for enhanced antifungal activity and bioavailability through oral administration for management of fungal infections. Chemistry and Physics of Lipids. 2020 Oct 1; 232:104953.
23. Dudhipala N, Veerabrahma K. Improved anti-hyperlipidemic activity of Rosuvastatin Calcium via lipid nanoparticles: Pharmacokinetic and pharmacodynamic evaluation. European Journal of Pharmaceutics and Biopharmaceutics. 2017 Jan 1;110:47-57.
24. Dudhipala N, Veerabrahma K. Candesartan cilexetil loaded solid lipid nanoparticles for oral delivery: characterization, pharmacokinetic and pharmacodynamic evaluation. Drug delivery. 2016 Feb 12; 23(2):395-404.
25. Dudhipala N, Puchchakayala G. Capecitabine lipid nanoparticles for anti-colon cancer activity in 1, 2-dimethylhydrazine-induced colon cancer: preparation, cytotoxic, pharmacokinetic, and pathological evaluation. Drug development and industrial pharmacy. 2018 Oct 3; 44(10):1572-82.
26. Müller RH, Radtke M, Wissing SA. Solid lipid nanoparticles (SLN) and nanostructured lipid carriers (NLC) in cosmetic and dermatological preparations. Advanced drug delivery reviews. 2002 Nov 1; 54:S131-55.
27. Mei Z, Chen H, Weng T, Yang Y, Yang X. Solid lipid nanoparticle and microemulsion for topical delivery of triptolide. European journal of pharmaceutics and biopharmaceutics. 2003 Sep 1; 56(2):189-96.
28. Wake PS, Kshirsagar MD. Compatibility study In-vitro drug release Study of Solid Lipid Nanoparticle Based Transdermal Drug Delivery System for Rasagiline Mesylate. Evaluation. 2017 Jun 28; 10:5.
29. Narendar D, Thirupathi G. Neuroprotective effect of ropinirole loaded lipid nanoparticles hydrogel for Parkinson's disease: preparation, in vitro, ex vivo, pharmacokinetic and pharmacodynamic evaluation. Pharmaceutics. 2020; 12(5):448.
30. Fuster J, Negro S, Salama A, Fernández-Carballido A, Marcianes P, Boeva L, Barcia E. HPLC-UV method development and validation for the quantification of ropinirole in new PLGA multiparticulate systems: Microspheres and nanoparticles. International journal of pharmaceutics. 2015 Aug 1; 491(1-2):310-7.
31. Dudhipala N, Janga KY, Gorre T. Comparative study of nisoldipine-loaded nanostructured lipid carriers and solid lipid nanoparticles for oral delivery: preparation, characterization, permeation and pharmacokinetic evaluation. Artificial cells, nanomedicine, and biotechnology. 2018 Nov 5; 46(sup2):616-25.
32. Dudhipala N, Veerabrahma K. Pharmacokinetic and pharmacodynamic studies of nisoldipine-loaded solid lipid nanoparticles developed by central composite design. Drug development and industrial pharmacy. 2015 Dec 2; 41(12):1968-77.
33. Gondrala UK, Dudhipala N, Kishan V. Preparation, characterization and in vivo evaluation of felodipine solid-lipid nanoparticles for improved oral bioavailability. Measurement. 2015; 10(10):2995-3002.
34. Dudhipala N, Janga KY. Lipid nanoparticles of zaleplon for improved oral delivery by Box–Behnken design: optimization, in vitro and in vivo evaluation. Drug development and industrial pharmacy. 2017 Jul 3; 43(7):1205-14.
35. Thirupathi G, Swetha E, Narendar D. Role of isradipine loaded solid lipid nanoparticles on the pharmacodynamic effect in rats. Drug research. 2017 Mar; 67(03):163-9.

36. Nagaraj K, Narendar D, Kishan V. Development of olmesartan medoxomil optimized nanosuspension using the Box–Behnken design to improve oral bioavailability. Drug development and industrial pharmacy. 2017 Jul 3; 43(7):1186-96.
37. Kakkar S, Pal Kaur I. A novel nanovesicular carrier system to deliver drug topically. Pharmaceutical development and technology. 2013 Jun 1; 18(3):673-85.
38. Palem CR, Gannu R, Doodipala N, Yamsani VV, Yamsani MR. Transmucosal delivery of domperidone from bilayered buccal patches: in vitro, ex vivo and in vivo characterization. Archives of pharmacal research. 2011 Oct; 34(10):1701-10.
39. Reddy AB, Reddy ND. Development of multiple-unit floating drug delivery system of clarithromycin: formulation, in vitro dissolution by modified dissolution apparatus, in vivo radiographic studies in human volunteers. Drug research. 2017 Jul; 67(07):412-8.
40. Yasir M, Chauhan I, Haji MJ, Tura AJ, Saxena PK. Formulation and evaluation of glyceryl behenate based solid lipid nanoparticles for the delivery of donepezil to brain through nasal route. Research Journal of Pharmacy and Technology. 2018 Jul 31; 11(7):2836-44.
41. Mahtab A, Anwar M, Mallick N, Naz Z, Jain GK, Ahmad FJ. Transungual delivery of ketoconazole nanoemulgel for the effective management of onychomycosis. AAPS PharmSciTech. 2016 Dec; 17(6):1477-90.
42. Ramasamy T, Khandasami US, Ruttala H, Shanmugam S. Development of solid lipid nanoparticles enriched hydrogels for topical delivery of anti-fungal agent. Macromolecular Research. 2012 Jul 1; 20(7):682-92.
43. Butreddy A, Dudhipala N, Janga KY, Gaddam RP. Lyophilization of small-molecule injectables: an industry perspective on formulation development, process optimization, scale-up challenges, and drug product quality attributes. AAPS PharmSciTech. 2020 Oct; 21(7):1-20.
44. Krishna VM, Kumar VB, Dudhipala N. In-situ intestinal absorption and pharmacokinetic investigations of carvedilol loaded supersaturated self-emulsifying drug system. Pharmaceutical nanotechnology. 2020 Jun 1; 8(3):207-24.
45. Pitta SK, Dudhipala N, Narala A, Veerabrahma K. Development of zolmitriptan transfersomes by Box–Behnken design for nasal delivery: in vitro and in vivo evaluation. Drug development and industrial pharmacy. 2018 Mar 4; 44(3):484-92.
46. Butreddy A, Narala A, Dudhipala N. Formulation and characterization of Liquid Crystalline Hydrogel of Agomelatin: In vitro and Ex vivo evaluation. Journal of Applied Pharmaceutical Science. 2015 Sep; 5(09):110-4.
47. Puglia C, Blasi P, Rizza L, Schoubben A, Bonina F, Rossi C, Ricci M. Lipid nanoparticles for prolonged topical delivery: an in vitro and in vivo investigation. International journal of pharmaceutics. 2008 Jun 5; 357(1-2):295-304.
48. Sweeney C, Dudhipala N, Thakkar R, Mehraj T, Marathe S, Gul W, ElSohly MA, Murphy B, Majumdar S. Effect of surfactant concentration and sterilization process on intraocular pressure–lowering activity of Δ 9-tetrahydrocannabinol-valine-hemisuccinate (NB1111) nanoemulsions. Drug delivery and translational research. 2020 Nov 9:1-2.
49. Dudhipala N. Influence of solid lipid nanoparticles on pharmaco-dynamic activity of poorly oral bioavailable drugs. International Journal of Pharmaceutical Sciences and Nanotechnology. 2020 Jul 11; 13(4):4979-83.
50. Tirumalesh C, Suram D, Dudhipala N, Banala N. Enhanced pharmacokinetic activity of Zotepine via nanostructured lipid carrier system in Wistar rats for oral application. Pharmaceutical nanotechnology. 2020 Apr 1; 8(2):148-60.
51. Youssef A, Dudhipala N, Majumdar S. Ciprofloxacin loaded nanostructured lipid carriers incorporated into in-situ gels to improve management of bacterial endophthalmitis. Pharmaceutics. 2020 Jun; 12(6):572.
52. Youssef AA, Cai C, Dudhipala N, Majumdar S. Design of Topical Ocular Ciprofloxacin Nanoemulsion for the Management of Bacterial Keratitis. Pharmaceuticals. 2021 Mar; 14(3):210.
53. Müller RH, Alexiev U, Sinambela P; Keck CM. Nanostructured Lipid Carriers (NLC): The Second Generation of Solid Lipid Nanoparticles. Percutaneous Penetration Enhancers Chemical Methods in Penetration Enhancement. 2016; 161–185: doi:10.1007/978-3-662-47862-2_11.
54. Suvarna G, Narender D, Kishan V. Preparation, characterization and in vivo evaluation of rosuvastatin calcium loaded solid lipid nanoparticles. Int J Pharm Sci Nanotech. 2015;9:2779-85.
55. Mehnert W, Mäder K. Solid lipid nanoparticles: production, characterization and applications. Advanced drug delivery reviews. 2012 Dec 1; 64:83-101.
56. Doodipala N, Palem C, Reddy S, Rao Y. Pharmaceutical development and clinical pharmacokinetic evaluation of gastroretentive floating matrix tablets of levofloxacin. Int J Pharm Sci Nanotech. 2011; 4(3):1461-7.
57. Doodipala NR, Sunil R, Rao M. Development of floating matrix tablets of Ofloxacin and Ornidazole in combined dosage form: in vitro and in vivo evaluation in healthy human volunteers. International Journal of Drug Delivery. 2012 Oct 1; 4(4):462.
58. Dudhipala N, Narala A, Janga KY, Bomma R. Amoxycillin trihydrate floating-bioadhesive drug delivery system for eradication of helicobacter pylori: preparation, in vitro and ex vivo evaluation. J Bioequiv Availab. 2016; 8(3):118-24.
59. Narendar D, Arjun N, Someshwar K, Rao YM. Quality by design approach for development and optimization of Quetiapine Fumarate effervescent floating matrix tablets for improved oral bioavailability. Journal of Pharmaceutical Investigation. 2016 Jun; 46(3):253-63.
60. Palem CR, Dudhipala N, Battu SK, Goda S, Repka MA, Yamsani MR. Combined dosage form of pioglitazone and felodipine as mucoadhesive pellets via hot melt extrusion for improved buccal delivery with application of quality by design approach. Journal of Drug Delivery Science and Technology. 2015 Dec 1; 30:209-19.
61. Palem CR, Dudhipala NR, Battu SK, Repka MA, Rao Yamsani M. Development, optimization and in vivo characterization of domperidone-controlled release hot-melt-extruded films for buccal delivery. Drug development and industrial pharmacy. 2016 Mar 3; 42(3):473-84.
62. Butreddy A, Dudhipala N. Enhancement of solubility and dissolution rate of trandolapril sustained release matrix tablets by liquisolid compact approach. Asian Journal of Pharmaceutic• Oct-Dec. 2015; 9(4):1.
63. Nagaraj B, Anusha K, Narendar D, Sushma P. Formulation and evaluation of microemulsion-based transdermal delivery of duloxetine hydrochloride. International Journal of Pharmaceutical Sciences and Nanotechnology. 2020 Jan 31; 13(1):4773-82.
64. Karri V, Butreddy A, Dudhipala N. Fabrication of efavirenz freeze dried nanocrystals: formulation, physicochemical characterization, in vitro and ex vivo evaluation. Advanced Science, Engineering and Medicine. 2015 May 1; 7(5):385-92.
65. Narendar D, Arjun N, Dinesh S, Karthik J. Biopharmaceutical and preclinical studies of efficient oral delivery of zaleplon as semisolid dispersions with self-emulsifying lipid surfactants. Int J Pharm Sci Nanotech. 2016; 9(1):1-8.
66. Kishan V, Sandeep V, Narendar D, Arjun N. Lacidipine loaded solid lipid nanoparticles for oral delivery: preparation, characterization and in vivo evaluation. International Journal of Pharmaceutical Sciences and Nanotechnology. 2016 Nov 30; 9(6):3524-30.
67. Banala N, Tirumalesh C, Suram D, Dudhipala N. Zotepine loaded lipid nanoparticles for oral delivery: preparation, characterization, and in vivo pharmacokinetic studies. Future Journal of Pharmaceutical Sciences. 2020; 6(1):37.
68. Kumar S, Somasundaram I. Development and Evaluation of Pramipexole Dihydrochloride and Piperine Loaded Chitosan Nanoparticles for Improved Treatment of Parkinson's Disease. Research Journal of Pharmacy and Technology. 2019; 12(12): 5822-5826.
69. Priya S, Jyothi D, James JP, Maxwell A. Formulation and Optimization of Ethosomes loaded with Ropinirole Hydrochloride: Application of quality by Design Approach. Research Journal of Pharmacy and Technology. 2020; 13(9):4339-4345.
70. Banala N, Cernam T, Suram D, Dudhipala N. Design, development and in vivo pharmacokinetic evaluation of zotepine loaded solid lipid nanoparticles for enhanced oral bioavailability. ACTA Pharmaceutica Sciencia. 2020.